Theoretical Foundations of Chemical Engineering, Vol. 39, No. 6, 2005, pp. 614–621.
Translated from Teoreticheskie Osnovy Khimicheskoi Tekhnologii, Vol. 39, No. 6, 2005, pp. 651–659.

Modeling of the Effect of pH on the Calcite Dissolution Kinetics

I. V. Dolgaleva*, I. G. Gorichev, A. D. Izotov***, and V. M. Stepanov***

** MAMI Moscow State Technical University,*
Bol'shaya Semenovskaya ul. 38, Moscow, 107023 Russia
*** Moscow Pedagogical State University,*
Malaya Pirogovskaya ul. 1, Moscow, 119882 Russia
**** Kurnakov Institute of General and Inorganic Chemistry, Russian Academy of Sciences,*
Leninskii pr. 31, Moscow, 119991 Russia
e-mail: Dolgaleva_Inna@mail.ru

Received April 18, 2005

Abstract—The kinetics and mechanism of calcite dissolution at various pH are investigated. A scheme of the ion distribution in various states of the medium is presented. The kinetic curves of dissolution are modeled, taking into account the structure of the electrical double layer and the acid–base characteristics of calcite.

The gas piped through gas pipelines always contains carbon dioxide, which causes corrosion of carbon steel. The steel corrosion rate is determined by the dissolution kinetics of calcium and iron carbonates, whose deposition stimulates carbonate corrosion in oil and gas pipelines [1, 2]. The calcite dissolution kinetics under various conditions (pH, CO_2 partial pressure, temperature, disc rotation frequency, etc.) was investigated previously [3–22].

The purpose of this work is to investigate the kinetic curves of calcite dissolution at various pH.

EXPERIMENTAL

Electrodes 5.3 cm in diameter were used, which were identified by IR spectroscopy. The calcite spectrum has a number of characteristic frequencies in the IR region at wave numbers of σ = 600, 713, 876, 1435, and 1795 m^{-1}. The wave numbers of characteristic frequencies in Raman spectroscopy are σ = 92, 105, 112, 154, 281, 712, and 1086 m^{-1}.

The dissolution kinetics was studied using a calcite disc electrode immersed in an electrolyte solution at various pH and rotation speed. The experiment was carried out at 21 ± 2°C. Samples were taken in the pH range of 2–14 every 10–30 min. The total specific dissolution rates W under various conditions were calculated by the chain-mechanism equation [23]

$$\alpha = 1 - \exp[-A\sinh(Wt)]. \quad (1)$$

The concentration of calcium ions in the solution was determined by potentiometric titration with a 0.1 N solution of EDTA disodium salt according to a published procedure [24].

The dependence of the calcite dissolution rate on the rotation speed of the disc electrode is illustrated in Fig. 1a. To calculate the dissolution rate constants and determine the kinetic contributions W_k and diffusion contributions W_d from the experimental data presented in Fig. 1b, we used the equation [6]

$$\frac{1}{W} = \frac{1}{W_k} + \frac{1}{W_d} = \frac{1}{z\mathrm{F}kc} + \frac{1.61\nu^{\frac{1}{6}}}{z\mathrm{F}cD^{2/3}\sqrt{\omega}} = a + b\frac{1}{\sqrt{\omega}}, \quad (2)$$

where z is the ion charge.

RESULTS AND DISCUSSION

Figure 2 shows the experimental results and literature data on the effect of pH. The kinetic curves demonstrate that, with an increase in pH, the rate decreases abruptly in the pH range of 2–5, is almost constant and is independent of the concentration of H^+ ions in the pH range of 5–10, and further decreases at pH above 10. In this context, it is necessary to theoretically describe the observed behavior.

Modeling of the Calcite Dissolution Kinetics according to the Classical Scheme

To model the effect of pH on the calcite dissolution kinetics, we chose the Hougen–Watson method, which is used to describe the dissolution specific rate as a function of various parameters and takes into account the concentrations of surface-active sites and intermediate particles that transfer into the solution [25]:

$$W = k\Gamma_a\Gamma_i. \quad (3)$$

To determine the dissolution rate, it is necessary to calculate the concentration of surface ions.

Figure 3 shows the distribution of surface-active ions, which affect the calcite dissolution rate at various

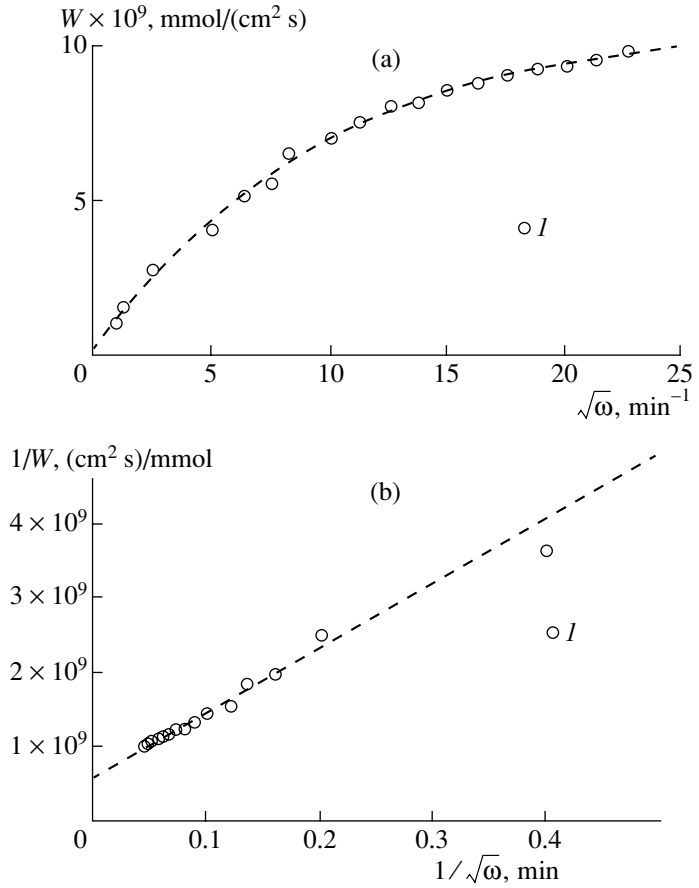

Fig. 1. Dependence of the rates of the (a) forward and (b) reverse reactions of calcite dissolution on the rotation speed of the disc electrode in a 0.7 M KCl solution (pH 8.4, T = 298 K), where point *1* represents the experimental data.

pH. The following particles can limit the dissolution rate:

$$H^+, \quad HCO_3^-, \quad CO_3^{2-}, \quad CaHCO_3^+,$$
$$CaCO_3^0, \quad CaOHCO_3^-.$$

To determine which of these particles on the calcite surface determines the rate, we modeled the pH dependence of the dissolution rate.

According to existing concepts, the concentration $[\Gamma(CaHCO_3^+)]$ of surface-active particles is expressed through the bulk concentration using the Langmuir equation [25]:

$$\Gamma(CaHCO_3^+) = \Gamma_\infty \frac{[CaHCO_3^+]}{[CaHCO_3^+] + K}. \quad (4)$$

In this case, the dependence of the dissolution rate on the $CaHCO_3^+$ concentration (if this rate is determined by the transfer of $CaHCO_3^+$ ions to the solution) can be expressed as

$$W = k\Gamma_\infty \frac{[CaHCO_3^+]}{[CaHCO_3^+] + K}. \quad (5)$$

To model the dissolution rate, we calculated the bulk concentrations of various particles as functions of pH.

For this purpose, it is necessary to solve the following equations:

(i) the mass balance equations:

for Ca^{2+} ions,

$$C(Ca^{2+}) = [Ca^{2+}] + [CaHCO_3^+] + [CaCO_3^0] + [CaOHCO_3^-] + [Ca(OH)_2^0] + [Ca(OH)_3^-]$$

for carbonate ions,

$$C(CO_3^{2-}) = [CO_2] + [CO_3^{2-}] + [HCO_3^-] + [H_2CO_3^0] + [CaHCO_3^+] + [CaOHCO_3^-] + [Ca(OH)_2CO_3^{2-}]$$

(ii) the equations of the equilibrium constants;

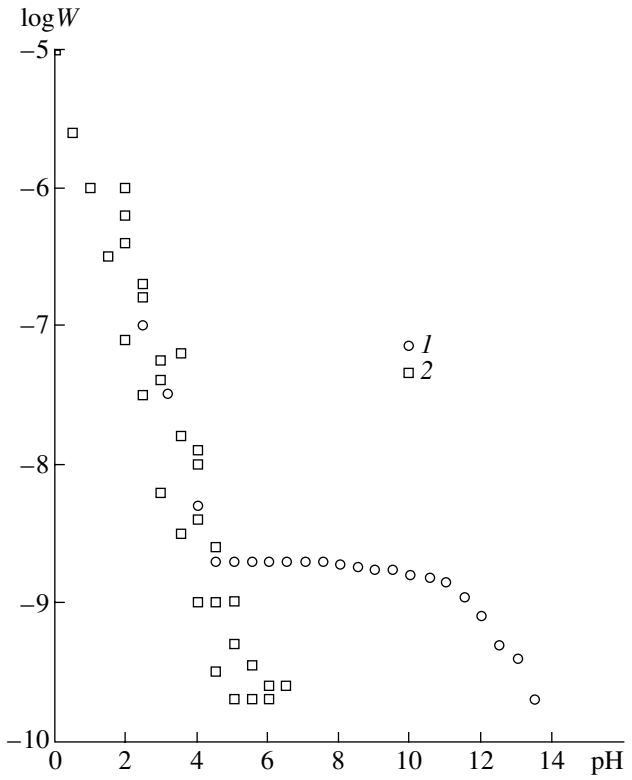

Fig. 2. pH dependence of the calcite dissolution rate: (*1*) experimental results and (*2*) published data [6, 8, 9, 12, 13, 21].

(iii) the equations of proton equilibrium and electroneutrality.

The results of simultaneously solving the equations for the particles considered are shown in Fig. 4. It follows from the particle distribution that all these particles can participate in dissolution. To select the rate-determining particles, let us use the equation of the dissolution rate for all the above particles:

$$W = k\Gamma_\infty \frac{[\mathrm{CaH}_n\mathrm{OH}_m(\mathrm{CO}_3^{2-})_p]}{[\mathrm{CaH}_n\mathrm{OH}_m(\mathrm{CO}_3^{2-})] + K}, \qquad (6)$$

where n, m, and p are the stoichiometric coefficients.

The modeling was performed using the standard program Mathcad 11.

Figure 4 shows that the surface-active particles at pH below 5 are H^+ and $CaHCO_3^+$ ions; in the pH range of 5–10, $CaOHCO_3^-$ ions; and at pH above 10, $Ca(OH)_2$ particles.

Thus, the total specific dissolution rate W is the sum of the rates:

$$W = W(\mathrm{H}^+) + W(\mathrm{HCO}_3^-) + W(\mathrm{Ca(OH)}_2^0) + W(\mathrm{CaOHCO}_3^-), \qquad (7)$$

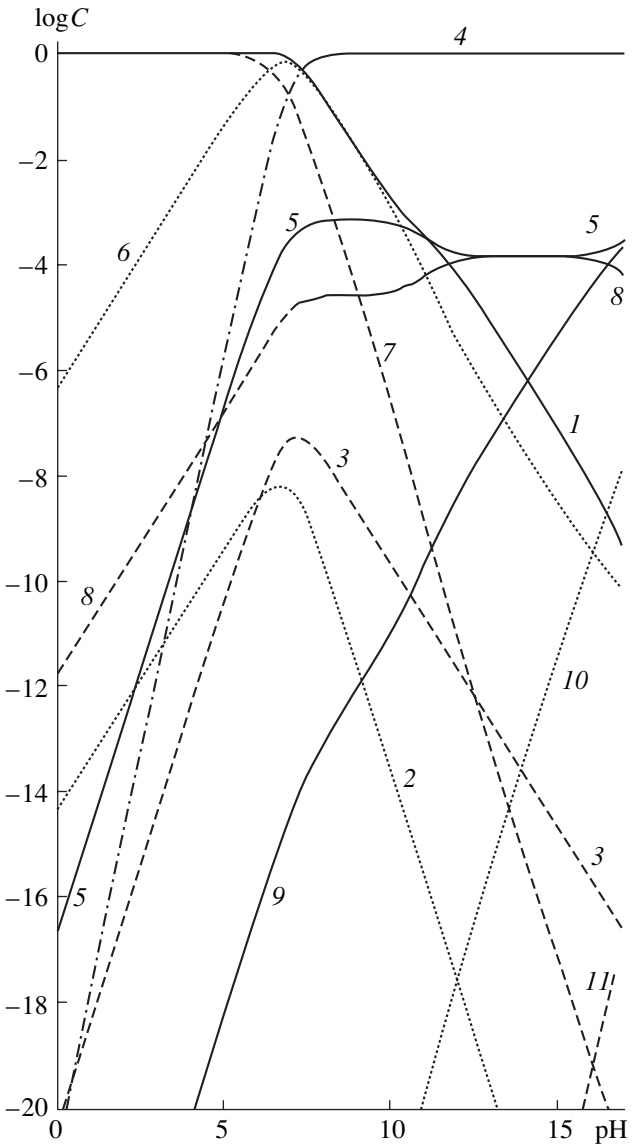

Fig. 3. pH dependence of the distribution of the relative fractions of various particles in calcite dissolution: (*1*) $\log[Ca^{2+}]$, (*2*) $\log[CaHCO_3^+]$, (*3*) $\log[CaCO_3^0]$, (*4*) $\log[CaOHCO_3^-]$, (*5*) $\log[H_2CO_3]$, (*6*) $\log[HCO_3^-]$, (*7*) $\log[CO_3^{2-}]$, (*8*) $\log[CaOH^+]$, (*9*) $\log[Ca(OH)_2]$, (*10*) $\log[Ca(OH)_3^-]$, and (*11*) $\log[Ca(OH)_4^{2-}]$.

where $W(H^+)$, $W(HCO_3^-)$, and $W(Ca(OH)_2^0)$ are the rates determined by the adsorption of hydrogen ions (pH below 5), hydrocarbonate ions (pH 5–8), and $Ca(OH)_2^0$ particles, respectively, on the calcite surface. The results of modeling the pH dependence of the calcite dissolution rate are also shown in Fig. 4.

The calculations showed that the pH dependence of the dissolution rate cannot be described using only one

sort of particles. At different pH, different sorts of adsorption particles determine the dissolution rate.

The modeling performed allows us to propose a scheme of calcite dissolution at various pH:

at pH 2–5,

$$CaCO_3 + H^+ \Leftrightarrow [CaHCO_3^+] \longrightarrow \text{dissolution products},$$

at pH 5–8,

$$CaCO_3 + HCO_3^- \Leftrightarrow Ca(HCO_3)_2^0 \longrightarrow \text{dissolution products},$$

at pH > 10,

$$CaCO_3 + OH^- \Leftrightarrow CaOHCO_3^- \longrightarrow \text{dissolution products}.$$

Modeling of the Calcite Dissolution Kinetics and the Structure of the Electrical Double Layer at the $CaCO_3$–Electrolyte Interface Using a Three-Layer Model

To describe the pH dependence of the calcite dissolution rate, we proposed an acid–base model (a three-layer model). This model takes into account the structure of the electrical double layer that emerges at the calcite–solution interface because of the adsorption and desorption of hydrogen ions [26–34].

The three-layer model is based on the Gram–Parsons theory and can be used to describe the $CaCO_3$–electrolyte interface.

The salt surface in the electrolyte solution is in dynamic equilibrium with various particles at the salt–electrolyte interface. In any salt–electrolyte systems, the solid surface acquires a charge q. The surface is charged both because of the selective adsorption of hydrogen ions H^+ or hydroxyl groups OH^- and because of the dissociation of surface groups. The ion adsorption on the salt surface is largely determined by the electrostatic interaction of ions.

In a symmetric electrolyte, e.g., KCl, at the calcite–electrolyte interface, the following equilibria can be established with ions H^+, K^+, OH^-, and Cl^- in the surface layer S [20]:

$$[S - CaCO_3H^+] \xrightarrow{K_1} [S - CaCO_3^0] + [H^+], \quad (8)$$

$$[S - CaCO_3^0] + [OH^+] \xrightarrow{K_2} [S - CaOHCO_3^-], \quad (9)$$

$$[S - CaCO_3 \circ H^+ \cdots Cl^-] \xrightarrow{K_3} [S - CaCO_3^0] + [Cl^-] + [H^+], \quad (10)$$

$$[S - CaCO_3^0] + [OH^-] + [K^+] \xrightarrow{K_4} [S - CaCO_3^0 \circ K^+ \cdots OH^-]. \quad (11)$$

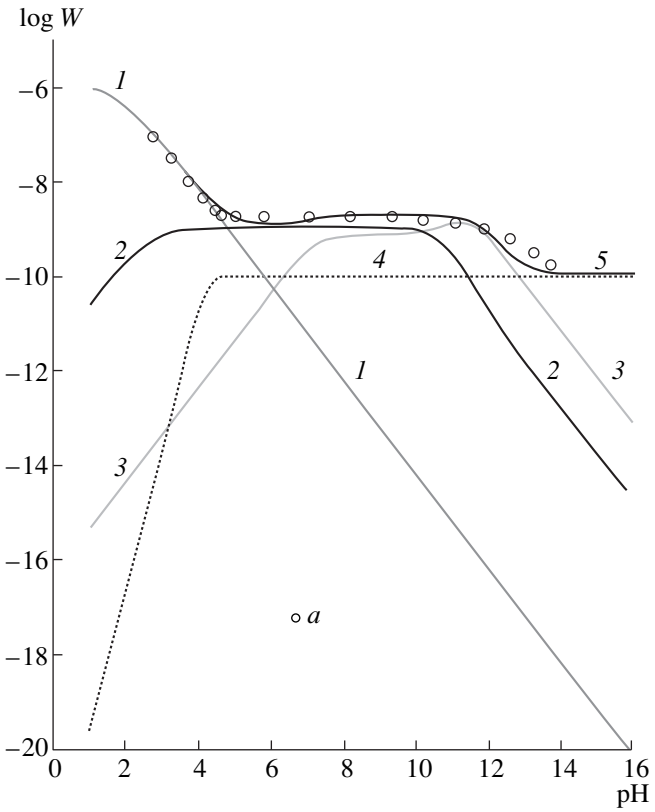

Fig. 4. pH dependence of the calcite dissolution rate according to the classical model where the rate is determined by the adsorption of (*1*) H^+ ions, (*2*) HCO_3^- ions, (*3*) $Ca(OH)_2^0$ particles, and (*4*) $CaOHCO_3^-$ ions on the calcite surface. Curve *5* is the total specific dissolution rate (the result of modeling), and point *a* represents the experimental data.

To calculate the equilibrium constants, it is necessary to know the electrostatic potential φ_0 and the charge q, which can be calculated using the three-layer model of the structure of the electrical double layer [34–36].

This model is based on a modern theory of the electrical double layer that was proposed by Gram and Parsons [20]. Let us consider its main provisions for the carbonate–electrolyte system. After immersion of calcite in an electrolyte, potential-determining ions H^+ and OH^- are adsorbed on the salt surface and impart a charge q to the salt surface. The potential jump φ_0 in the ion electrical double layer is counted from the potential of zero charge (i.e., φ_0 is taken to be zero at pH_0).

The model of the electrical double layer can be represented as follows.

(i) Between the carbonate surface and the plane passing through the centers of dehydrated ions (the inner Helmholtz plane), there is a potential jump, $\varphi_0 - \varphi_1$, and the total charge in this plane is q_1.

(ii) Between the inner and the outer Helmholtz planes, there is also a potential jump, $\psi_1 - \psi_2$. The outer Helmholtz plane is determined by the minimal distance of the electrical centers of hydrated ions to the salt surface (its average potential ψ_2 is counted from the bulk of the solution).

(iii) The potential jump between the outer plane and the bulk of the solution is ψ_2.

The charge q is balanced by the charge q_1 of counterions on the inner Helmholtz plane and by the total charge q_2 of the diffusion layer. Thus,

$$\varphi_0 = (\varphi_0 - \psi_1) + (\psi_1 - \psi_2) + \psi_2. \quad (12)$$

For the average electrostatic potential on the inner Helmholtz plane, we obtain

$$\psi_1 = \varphi_0 - \frac{q}{K_{01}}, \quad (13)$$

or

$$\varphi_0 - \psi_1 = q/K_{01}, \quad (14)$$

where $K_{01} = q/(\varphi_0 - \psi_1)$ is the integral capacitance of the capacitor formed by the salt surface and the inner Helmholtz plane.

The average potential of the outer Helmholtz plane with allowance for the fact that $q_2 = -(q + q_1)$ is

$$\psi_2 = \psi_1 + \frac{q_2}{K_{12}}, \quad (15)$$

or

$$\psi_1 - \psi_2 = -q_2/K_{12} = (q + q_1)/K_{12}, \quad (16)$$

where K_{12} is the integral capacitance of the capacitor formed by the inner and the outer Helmholtz planes. Using Eqs. (12)–(14), we find the potential jump between the salt surface and the outer Helmholtz plane:

$$\varphi_0 - \psi_2 = \frac{q}{K_{02}} - \frac{q_1}{K_{12}}, \quad (17)$$

where $1/K_{02} = 1/K_{01} + 1/K_{12}$.

Using the concepts of the electrical double layer and the acid–base properties of calcite, we can describe the dissolution rate by the equations related to two adsorption isotherms for hydrogen ions.

The concentration of adsorption particles at any distance from the salt surface depends on the potential ψ_1 at this point and is determined by the Boltzmann equation

$$\left\lfloor \mathrm{H}_i^+ \right\rfloor = \left\lfloor \mathrm{H}_i^+ \right\rfloor \exp(-z\mathrm{F}\psi_1/RT). \quad (18)$$

Thus, to describe the ion part of the electrical double layer and to calculate the surface concentrations of various particles at the calcite–electrolyte interface, the following parameters should be known: pK_1, pK_2, pK_3, pK_4, N_S, K_{01}, and K_{02}, which were determined from the pH dependence of the electrokinetic potential ζ [37, 38].

The calculation of equilibrium constants (8)–(11) consisted in the determination of the charge q_2 in the outer Helmholtz region using the equation [20]

$$q_2 = -2A_0\sqrt{C_{\mathrm{el}}}\sinh(\zeta\mathrm{F}/2RT), \quad (19)$$

where $A_0 = 5.85 \times 10^{-6}$ C/cm^2.

The determination of pH_0 consisted in finding the pH at $q_2 = 0$.

The charges q and q_1 at the calcite–electrolyte interface on the inner Helmholtz plane were calculated by the equation

$$q = -(q_1 + q_2) - \left\{ 2A_1 C_{\mathrm{el}} \sinh\left[\left(\frac{q\mathrm{F}}{K_{01}RT} \right) + \ln\frac{[\mathrm{H}^+]_0}{[\mathrm{H}^+]} \right] + q_2 \right\}, \quad (20)$$

where $A_1 = 39.2 \times 10^{-6}$ C/cm^2.

The potential jump φ_0 at the calcite–electrolyte interface was calculated by the equation

$$\varphi_0 = \frac{RT}{\mathrm{F}} \left\{ \ln\frac{[\mathrm{H}^+]}{[\mathrm{H}^+]_0} + \operatorname{arcsinh}(A_2 q_2) \right\}, \quad (21)$$

where $A_2 = 10^6$ C/cm^2.

Using the found parameters q and φ_0, we can calculate the constants $pK_1 - pK_2$ by the equation [35, 36]

$$q = -N_S F \frac{\frac{pK_1}{pK_3} C_{\mathrm{el}} \sinh[(\varphi_0 - \psi_1)\mathrm{F}/RT] + \sinh(\varphi_0\mathrm{F}/RT)}{\frac{pK_1}{pK_3} C_{\mathrm{el}} \cosh[(\varphi_0 - \psi_1)\mathrm{F}/RT] + \cosh(\varphi_0\mathrm{F}/RT) + \frac{pK_1}{2[\mathrm{H}^+]_0}}. \quad (22)$$

The values of these parameters are the following:

$$pK_1 = 5.2 \quad N_s = 6 \times 10^{-5}$$

$$pK_2 = 9.1 \quad K_{01} = 100$$

$$pK_3 = 7.4 \quad \mathrm{pH}_0 = 7.15$$

$$pK_4 = 6.9.$$

The results of calculating the calcite surface charge as a function of pH are shown in Fig. 5, which suggests

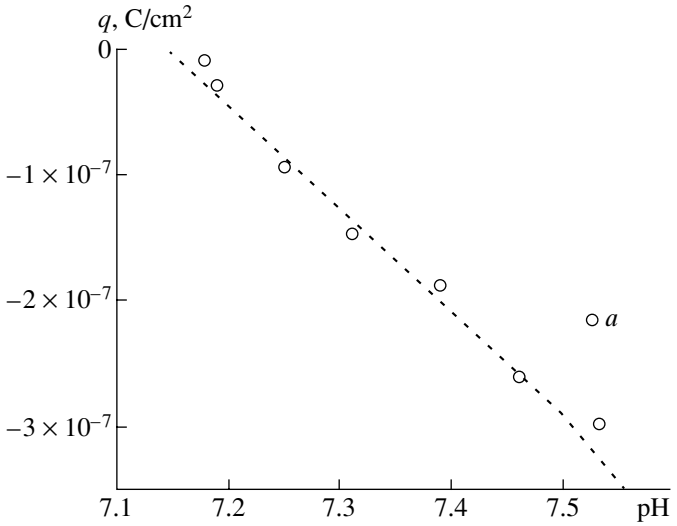

Fig. 5. Charge of the calcite surface at the solid–solution interface versus the pH of a 0.015 M KCl solution. The line represents the results of calculation by Eq. (22), and point *a*, the experimental calcite charge value determined from the dependence of the electrokinetic potential on the pH of the solution.

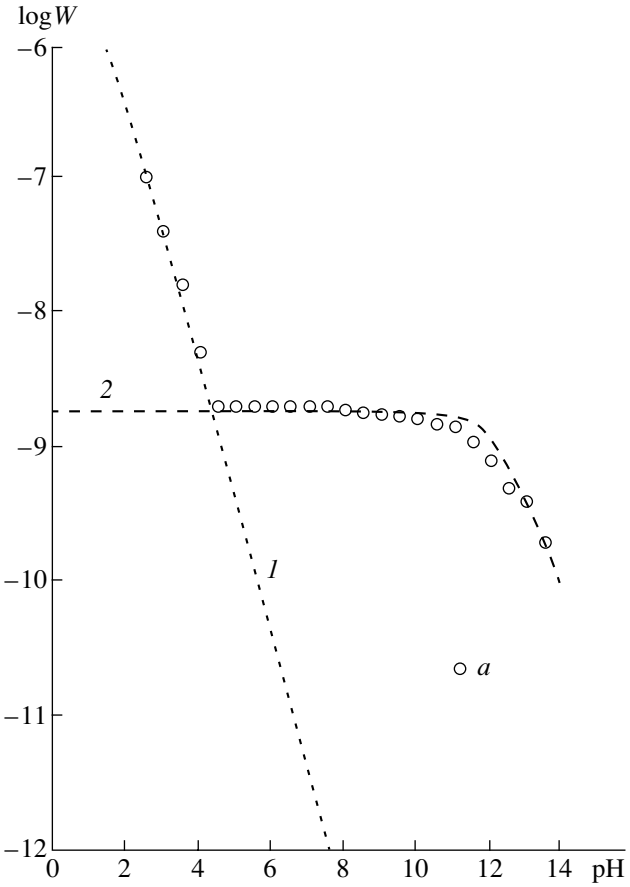

Fig. 6. pH dependence of the calcite dissolution rate as calculated according to the acid–base model from (*1*) Eq. (23) and (*2*) Eq. (24); point *a* represents the experimental data.

that the calcite dissolution rate is determined by the calcite surface charge.

Using the found charge distribution, it is possible to describe the pH dependence of the dissolution rate. The pH dependence of the calcite dissolution rate according to the acid–base model is illustrated in Fig. 6. In the acidic region, this dependence is described by the equation

$$W_1 = W_{01}\left[\frac{[H^+]}{[H^+] + K_{a1}}\right], \qquad (23)$$

where $W_{01} = 10^{-5.7}$ and $K_{a1} = 10^{-1.25}$ is the experimental value of adsorption of H^+ ions.

The equilibrium constant K_{eq} was determined from the formula $K_{eq} = pH_0 - pK_1$.

In the basic region, the dependence of the dissolution rate on the hydrogen ion concentration is described by the equation

$$W_2 = W_{02}\left[\frac{[H^+]}{[H^+] + K_{a2}}\right] = W_{02}\left[\frac{1}{K_{a3}[OH^-]}\right], \qquad (24)$$

where $W_{02} = 10^{-8.75}$ and $K_{a2} = 10^{-11.95}$ and $K_{a3} = 10^{2.0}$ are the experimental values of the ion adsorption. The equilibrium constant was found from the formula $K_{eq} = pH_0 - pK_2$.

Note that the forms of Eqs. (23) and (24), which describe the adsorption of H^+ and OH^- ions, are identical. The approach proposed allowed us to explain the effect of pH on the dissolution rate from the standpoint of the structure of the electrical double layer.

The results obtained suggest that the calcite dissolution kinetics is determined by the rate of formation of acidic surface compounds, e.g., $(CaHCO_3)^+$, and basic intermediate compounds, e.g., $(CaOHCO_3)^-$.

The acid–base mechanism of $CaCO_3$ dissolution enabled us to propose the following scheme:

in the acidic region ($2 < pH < 4.7$),

$$CaCO_3 + H^+ \Leftrightarrow CaHCO_3^+ \longrightarrow Ca^{2+} + HCO_3^-;$$

in the basic region ($6.7 < pH < 13$),

$$CaCO_3 + OH^- \Leftrightarrow (CaOH^+ \cdots CO_3^{2-})$$
$$\longrightarrow \text{dissolution products.}$$

The proposed approach is consistent with the classical models described above.

NOTATION

A—quantity proportional to the number of active centers;

A_0, A_1, A_2—constants of various models of the electrical double layer;

a, b, d—empirical constants;

C_{el}—electrolyte concentration, mol/l;

D—diffusivity, cm^2/s;

F = 96 485 C/mol—Faraday number;

$[H^+]$, $[OH^-]$—bulk concentrations of hydrogen ions and hydroxyl groups, respectively, mol/l;

K, K_1, K_2, K_3, K_4—constants of adsorption equilibria;

K_{01}, K_{02}, K_{12}—integral capacitances of the condenser formed by the inner and outer planes, $\mu F/cm^2$;

k—constant of kinetic processes;

N_s—total concentration of all particles adsorbed on the salt surface, mol/l;

P_{CO_2}—carbon dioxide partial pressure, Pa;

pK_1, pK_2, pK_3, pK_4—constants of acid–base equilibria;

q, q_1, q_2—charges of the planes passing through the salt surface and the inner and outer Helmholtz planes, C/cm^2;

S—total surface area, cm^2;

$[S-CaCO_3H^+]$, $[S-CaCO_3^0]$, $[S-CaCO_3 \circ H^+\cdots Cl^-]$—concentrations of various particles adsorbed on the surface;

t—time, s;

V—solution volume, l;

W—total specific dissolution rate, $mmol/(s\ cm^2)$;

W_{01}, W_{02}—specific dissolution rates, $mmol/(s\ cm^2)$;

W_d—rate of the diffusion process, $mmol/(s\ cm^2)$;

W_k—rate of the kinetic process, $mmol/(s\ cm^2)$;

$W(H^+)$, $W(HCO_3^-)$, $W(Ca(OH)_2^0)$, $W(CaOHCO_3^-)$—partial dissolution rates for various particles, $mmol/(s\ cm^2)$;

z—ion charge;

α—fraction of the dissolved substance;

Γ—surface concentration of particles, mol/cm^2;

δ—thickness of the diffusion layer, cm;

ζ—electrokinetic potential, V;

ν—kinematic viscosity of the solution, m^2/s;

σ—wave number, m^{-1};

φ_0—potential jump with respect to the bulk of the solution, V;

ψ_1, ψ_2—potentials on the inner and outer Helmholtz planes, V;

ω—rotation speed of the disc electrode, min^{-1}.

SUBSCRIPTS AND SUPERSCRIPTS

a—active centers;

i—surface ions;

∞—limiting concentration.

REFERENCES

1. Legrand, L., Savoye, S., Chausse, A., and Messina, R., Study of Oxidation Products Formed on Iron in Solutions Containing Bicarbonate/Carbonate, *Electrochim. Acta*, 2000, vol. 46, p. 111.
2. Videm, K. and Dugstad, A., Corrosion of Carbon Steel in an Aqueous Carbon Dioxide Environment, *Mater. Perform.*, 1989, vol. 28, no. 4, p. 46.
3. Sjöberg, E.L., A Fundamental Equation for Calcite Dissolution Kinetics, *Geochim. Cosmochim. Acta*, 1976, vol. 40, p. 441.
4. Jensen, D.L., The Solubility of Rhodochrosite ($MnCO_3$) and Siderite ($FeCO_3$) in Anaerobic Aquatic Environments, *Appl. Geochem.*, 2002, vol. 17, p. 503.
5. Lim, T., Hwang, E.R., and Ha, H., Effects of Temperature and Partial Pressure of CO_2/O_2 on Corrosion Behaviour of Stainless-Steel in Molten Li/Na Carbonate Salt, *J. Power Sources,* 2000, vol. 89, p. 1.
6. Fredd, C.N. and Fogler, H.S., The Kinetics of Calcite Dissolution in Acetic Acid Solutions, *Chem. Eng. Sci.*, 1998, vol. 53, p. 3863.
7. Liang, Y., Baer, D.R., and McCoy, J.M., Dissolution Kinetics at the Calcite–Water Interface, *Geochim. Cosmochim. Acta*, 1996, vol. 60, p. 4883.
8. Sjöberg, E.L. and Rickard, D., Calcite Dissolution Kinetics: Surface Speciation and the Origin of the Variable pH Dependence, *Chem. Geol.*, 1984, vol. 42, p. 119.
9. Sjöberg, E.L. and Rickard, D., Temperature Dependence of Calcite Dissolution Kinetics between 1 and 62°C at pH 2.7 to 8.4 in Aqueous Solutions, *Geochim. Cosmochim. Acta*, 1984, vol. 48, p. 485.
10. Morse, J.W., The Kinetics of Calcium Carbonate Dissolution and Precipitation, in *Carbonates: Mineralogy and Chemistry*, Reeder, R.J., Ed., vol. 11 of *Reviews in Mineralogy, Mineralogical Society of America*, 1983, p. 227.
11. Rickard, D. and Sjöberg, E.L., Mixed Kinetic Control of Calcite Dissolution Rates, *Am. J. Sci.*, 1983, vol. 283, p. 815.
12. Plummer, L.N., Wigley, T.M.L., and Parkhurst, D.L., A Critical Review of the Kinetics of Calcite Dissolution and Precipitation, in *Chemical Modelling of Aqueous Systems*, Jenne, E.A., Ed., *Am. Chem. Soc. Symp. Ser.*, 1979, vol. 36, p. 538.
13. Plummer, L.N., Wigley, T.M.L., and Parkhurst, D.L., The Kinetics of Calcite Dissolution in CO_2–Water Systems at 5–10°C and 0.0–1.0 atm CO_2, *Am. J. Sci.*, 1978, vol. 278, p. 179.
14. Sjöberg, E.L., Kinetics and Mechanism of Calcite Dissolution in Aqueous Solutions at Low Temperatures, *Stockholm Contrib. Geol.*, 1978, vol. 32, p. 1.
15. Plummer, L.N. and Wigley, T.M.L., The Dissolution of Calcite in CO_2-Saturated Solutions at 25°C and One Atmosphere Total Pressure, *Geochim. Cosmochim. Acta*, 1976, vol. 40, p. 191.

16. Sjöberg, E.L., A Fundamental Equation for Calcite Dissolution Kinetics, *Geochim. Cosmochim. Acta*, 1976, vol. 40, p. 441.
17. Morse, J.W., Dissolution Kinetics of Calcium Carbonate in Seawater: 3. A New Method for the Study of Carbonate Reaction Kinetics, *Am. J. Sci.*, 1974, vol. 274, p. 97.
18. Tarasevich, M.R., Khrushcheva, E.I., and Filinovskii, V.Yu., *Vrashchayushchiisya diskovyi elektrod s kol'tsom* (Rotating-Ring Disk Electrode), Moscow: Nauka, 1987.
19. Pleskov, Yu.V. and Filinovskii, V.Yu., *Vrashchayushchiisya diskovyi elektrod* (Rotating Disc Electrode), Moscow: Nauka, 1972.
20. Damaskin, B.B. and Petrii, O.A., *Vvedenie v elektrokhimicheskuyu kinetiku* (Introduction to Electrochemical Kinetics), Moscow: Vysshaya Shkola, 1983.
21. Fredd, C.N. and Fogler, H.S., The Influence of Chelating Agents on the Kinetics of Calcite Dissolution, *J. Colloid Interface Sci.*, 1998, vol. 204, p. 187.
22. Hales, B. and Emerson, S., Evidence in Support of First-Order Dissolution Kinetics of Calcite in Seawater, *Earth Planet. Sci. Lett.*, 1997, vol. 148, p. 317.
23. Gorichev, I.G., Kutepov A.M., Gorichev, A.I., Izotov, A.D., *Kinetika i mekhanizm rastvoreniya oksidov i gidroksidov zheleza v kislykh sredakh* (Kinetics and Mechanism of Dissolution of Iron Oxides and Hydroxides in Acidic Media), Moscow: Ross. Univ. Druzhby Narodov, 1999.
24. Charlot, G., *Les methodes de la chimie analytique*, Paris: Masson, 1961. Translated under the title *Metody analiticheskoi khimii*, Moscow: Khimiya, 1965.
25. Bezdenezhnykh, A.A., *Inzhenernye metody sostavleniya uravnenii skorostei reaktsii i rascheta kineticheskikh konstant* (Engineering Methods for Formulating the Reaction Rate Equations and Calculating the Kinetic Constants), Leningrad: Khimiya, 1973.
26. Wiese, G.R., James, R.O., Yates, D.E., and Healy, T.W., Electrochemistry of the Colloid/Water Interface, *Int. Rev. Sci.*,, 1976, vol. 6, p. 53.
27. Westall, J. and Hohl, H., A Comparison of Electrostatic Models for the Oxide/Solution Interface, *Adv. Colloid. Interface Sci.,* 1980, vol. 12, no. 2, p. 265.
28. Davis, J.A., James, R.D., and Leckie, J.O., Surface Ionization and Complexation at the Oxide/Water Interface, *J. Colloid Interface Sci.*, 1978, vol. 63, no. 3, p. 480.
29. Davis, J.A. and Leckie, J.O., Surface Properties of Amorphous Iron Oxyhydroxide and Adsorption of Metal Ions, *J. Colloid Interface Sci.*, 1978, vol. 67, no. 1, p. 90.
30. Davis, J.A. and Leckie, J.O., Adsorption of Anions, *J. Colloid Interface Sci.*, 1980, vol. 74, no. 1, p. 32.
31. Hayes, K.F., Papelis, C., and Leckie, J.O., Modeling Ionic Strength Effects on Anion Adsorption at Hydrous Oxide/Solution Interfaces, *J. Colloid Interface Sci.*, 1988, vol. 125, no. 2, p. 717.
32. Hayes, K.F. and Leckie, J.O., Modeling Ionic Strength Effects on Cation Adsorption at Hydrous Oxide/Solution Interfaces, *J. Colloid Interface Sci.*, 1987, vol. 115, no. 2, p. 564.
33. Barrow, N.J. and Bowden, J.W., A Composition of Models for Describing the Adsorption of Anions on a Variable Change Mineral Surface, *J. Colloid Interface Sci.*, 1987, vol. 119, no. 1, p. 236.
34. Barrow, N.J., Effect of Surface Heterogeneity on Ion Adsorption by Metal Oxide and by Soils, *Langmuir*, 1993, vol. 9, no. 10, p. 2606.
35. Gorichev, I.G., Batrakov, V.V., and Shaplygin, I.S., Complexation on the Surface of Iron Hydroxides: I. Investigation Methods and Model Description of the Acid–Base Properties at the Iron Oxide–Electrolyte Interface, *Neorg. Mater.*, 1994, vol. 30, no. 10, p. 330.
36. Gorichev, I.G., Batrakov, V.V., and Shaplygin, I.S., Complexation on the Surface of Iron Hydroxides: II. Experimental Data on Ion Adsorption and Surface Complexation, *Neorg. Mater.*, 1994, vol. 30, no. 10, p. 346.
37. Moulin, P. and Roques, H., Zeta Potential Measurement of Calcium Carbonate, *J. Colloid Interface Sci.*, 2003, vol. 261, p. 115.
38. Huang, Y.C., Fowkes, F.M., Lloyd, T.B., and Sanders, N.D., Adsorption of Calcium Ions from Calcium Chloride Solutions onto Calcium Carbonate Particles, *Langmuir*, 1991, vol. 7, no. 8, p. 1742.